JOURNAL OF PROPULSION AND POWER
Vol. 23, No. 4, July–August 2007

Reaction Propagation of Four Nanoscale Energetic Composites (Al/MoO_3, Al/WO_3, Al/CuO, and Bi_2O_3)

V. Eric Sanders,* Blaine W. Asay,† Timothy J. Foley,† Bryce C. Tappan,† Adam N. Pacheco,* and Steven F. Son‡
Los Alamos National Laboratory, Los Alamos, New Mexico 87545

DOI: 10.2514/1.26089

Nanoscale composite energetics (also known as metastable intermolecular composites) represent an exciting new class of energetic materials. Nanoscale thermites are examples of these materials. The nanoscale thermites studied consist of a metal and metal oxide with particle sizes in the 30–200 nm range. They have potential for use in a wide range of applications. The modes of combustion and reaction behavior of these materials are not yet well understood. This investigation considers four different nanoaluminum/metal–oxide composites. The same nanoscale aluminum was used for each composite. The metal oxides used were molybdenum oxide (MoO_3), tungsten oxide (WO_3), copper oxide (CuO), and bismuth oxide (Bi_2O_3). The reaction performance was quantified by the pressure output and propagation velocity using unconfined (or open burn) and confined (burn tube) experiments. We examine the optimization of each composite in terms of pressure output and propagaton speed (or burn rate) for the open burn experiment. We find that there is a correlation between the maximum pressure output and optimum propagation speed (or burn rate). Equilibrium calculations are used to interpret these results. We find that the propagation speed depends on the gas production and also on the thermodynamic state of the products. This suggests that condensing gases or solidifying liquids could greatly enhance heat transfer. We also vary the density of these composites and examine the change in performance. Although the propagation wave is likely supersonic with respect to the mixture sound speed, the propagation speed decreases with density. This behavior is opposite of classical detonation in which propagation (detonation) speed increases with density. This result indicates that the propagation mechanism may differ fundamentally from classical detonations.

I. Introduction

RECENT developments in the production of nanoscale materials have led to a new class of energetic materials (EM) commonly referred to as nanoscale composite energetic materials, or simply nanoenergetics. These materials are also called metastable intermolecular composites (MIC) and include nanoscale thermites. This class of materials uses nanosized (typically tens of nanometers) particles of reactants to produce dramatic changes in combustion behavior. Nanoscale thermites are composed of nanosized metals and metal oxides instead of the micron sized constituents used in conventional thermites. The reduction of particle size and corresponding increased surface area effectively reduces the barriers between reactants while increasing the homogeneity of the mixture. Consequently, combustion occurs much faster with these materials compared to micron-scale thermite powder reactions. This results in dramatically increased propagation speeds and ignition sensitivity while maintaining high combustion temperatures. Typically, reaction rates of nanoscale thermites are orders of magnitude faster than traditional thermites as inferred from observed propagation speeds and reaction cell results [1].

There are a number of factors that can potentially change the combustion of these systems in addition to particle size. Additional factors include reactant species, reaction kinetics, powder density, oxide layer thickness (such as the passivation layer on Al particles), and particle morphology. In addition, the introduction of other ingredients such as binders or gas producing agents into the system can dramatically affect properties and performance. The rapid combustion and the ability to engineer or tailor these composites lends to their possible use in a wide range of applications. For example, these materials are currently being investigated for use as a replacement for lead-based percussion and electric primers.

The primary mode of reaction propagation in these materials is not yet thoroughly understood. Previous work [2] suggests convection as the likely dominant process in low-density configurations but also reports a possible transition to conduction dominant combustion (or normal deflagration) at higher densities. The convective mode was further explored by Asay et al. [3]. Radiant transport may also contribute but the extent of this contribution is believed to be relatively small as demonstrated by their results [3]. Specifically, they showed that using infrared transparent barriers would effectively stop the propagation of reaction across those barriers. The contribution, if any, of shock or acoustic effects on the reaction propagation of these materials has not been as thoroughly examined.

Here, we report details of several experimental techniques used on four different metal/metal–oxide systems. We compare the reaction propagation behavior of the four composites. A focus of this study is the density and contrasting the behavior of the different composite systems.

II. Experimental

The materials used in this investigation along with their properties are listed in Table 1. (Care should be exercised when handling the formulated composites because of their sensitivity to impact, spark, and friction.) The same nanoaluminum (nominally 80 nm, 88% active Al content, 12% Al_2O_3) was used in all four composites. As the table illustrates, there are differences in the size and morphology of the four oxides. These differences will potentially affect the reactivity of each composite and limit our ability to conduct a more direct comparison of the four systems, but the data still reveal insight into each oxide's behavior and the characteristics of nanoscale composites in general. The Bi_2O_3 used in this study had a particle size of approximately 2 μm while the other oxides were in the

Received 22 June 2006; revision received 29 March 2007; accepted for publication 30 March 2007.

*Research Technician, High Explosives Science and Technology.
†Technical Staff Member, High Explosives Science and Technology.
‡Associate Professor, Currently at Purdue University, West Lafayette, IN, 47907. AIAA Member.

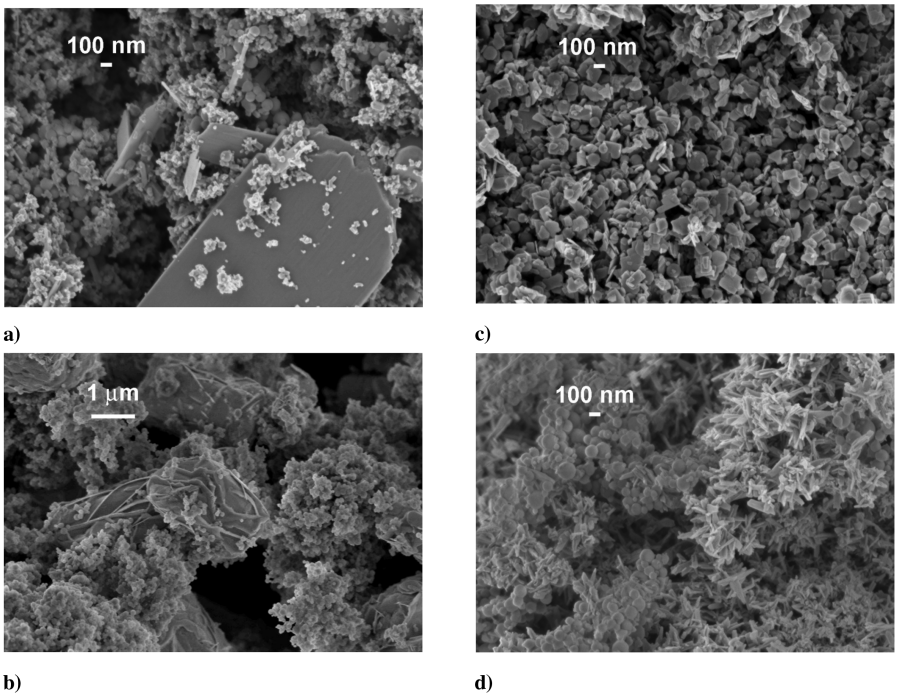

Fig. 1 a) SEM of Al/MoO_3 composite, 25KX magnification. b) SEM of Al/Bi_2O_3 composite, 10KX magnification. c) SEM of Al/WO_3 composite, 25KX magnification. d) SEM of Al/CuO composite, 25KX magnification.

nanometer range. This size was chosen because of the extreme ignition sensitivity of composites made with nanosized Bi_2O_3. Figures 1a–1d are scanning electron micrographs (SEMs) of the four tested composites and show the differences in morphology. Although not a quantitative measure, these SEM images reveal the morphological differences of each mixture. Mixing can greatly affect the reactivity of these materials [4,5], however, for this study the effects of different mixing techniques were not investigated. For the purpose of this study, the composites were mixed in solution using ultrasonic mixing. In the case of MoO_3 and CuO, hexane was used as the solvent. For WO_3 and Bi_2O_3, isopropanol was used. Isopropanol is a polar liquid, which greatly improves mixing of particles of disparate densities. We minimize the time of exposure of the aluminum with the isopropanol to avoid significant oxidation. Very little oxidation occurs for the exposure times used (verified by measuring active Al content in separate experiments), but if exposed for longer times significant oxidation can occur. Following sonication, the mixtures were placed onto a steel pan and allowed to dry on a hot plate at ~48°C. A 355 μm mesh sieve was then used to break up large agglomerations in the composites. The WO_3 was in its hydrated form and was synthesized following a literature procedure [6]. The other materials were used as received from the manufacturer (see Table 1).

Several experimental techniques were used to characterize and contrast the reaction behavior of these materials. These experiments included a closed bomb pressure test, unconfined velocity test (open tray), and instrumented tubes in which both propagation speed and pressure are measured along the length of a tube. The term ignition front refers to the front edge of the luminous part of the reaction where light is first detected.

A. Pressure Cell Experiments

Closed bomb pressure measurements were made with the four composite systems. In this experiment, a loose powder sample was placed into the pressure cell and ignited using an Nd:YAG laser via an optical fiber. The amount of energy delivered to the sample was approximately 9 mJ. For optimization experiments, the sample size was determined by the volume of the sample holder (0.15 cm^3). Therefore, the mass of each sample varied between the different composites but was held constant for each test of a specific composite. Upon ignition of the sample, pressure measurements were made using two piezoelectric gauges with response times of <1 μs (PCB Piezotronics, Inc., models 113A22 and 113A23). Two gauges are used for redundancy. The resulting pressure was recorded via a signal conditioning amplifier onto a Tektronix digital oscilloscope. A more detailed description of the pressure cell can be found in previous work [7].

B. Open Tray Burn Experiments

Propagation speed was measured by spreading small samples of loose powder evenly into a groove machined into a metal tray and igniting the sample at one end. The metal tray is designed with two small holes in the bottom of the groove separated by a distance of 20 mm. The groove allows for a uniform cross section of the sample. Aligned with these holes are optical fibers coupled to photodiodes. The response times of the photodiodes are about 1 ns (Thorlabs DET-210). The time of arrival of light produced by the reaction is recorded onto a digital oscilloscope as the reaction front propagates past the optical fibers. In these experiments, samples were ignited using a piezoelectric igniter. A more detailed experimental description is

Table 1 Materials studied

Constituent	Supplier	Surface area, m^2/g	Nominal particle size and morphology
Aluminum	Nanotechnologies, Inc.	27.7[a]	80 nm spherical
Bi_2O_3	Skylighter, Inc.	0.269[b]	25 μm rod
CuO	Technanogy	31.3[a]	~21 nm × 100 nm rod
MoO_3	Technanogy	64[a]	~30 nm × 200 nm sheet
WO_3	LANL	27.1 [12]	100 nm × 20 nm platelet [12]

[a]Measured by manufacturer. [b]Calculated.

provided elsewhere [2]. Similar experiments [8] have been performed in other laboratories using a modified version of the Los Alamos National Laboratory (LANL) open burn apparatus. They found that the use of baffles improved repeatability. In the experiments reported here, five in-line baffles were used.

C. Instrumented Burn Tube Experiments

The instrumented burn tube experiment, originally designed by Bockman et al. [9], was used to study reaction propagation in a more one-dimensional cylindrical geometry. Several modifications have been made to the original design which have allowed for the experiment to be used in a number of different configurations. Our experiment consisted of an acrylic tube of 3.2 mm inner diam, 6.4 mm outer diam, and lengths of either 88.9 or 101.6 mm. The tube was placed inside a block that is configured with six pressure gauges and six light fibers placed on opposing sides of the block and at 10 mm intervals along the length of the tube. The blocks used were made of acrylic, polycarbonate, or stainless steel. The acrylic and polycarbonate blocks were used to allow recording of the event with digital photography. Tubes were typically loaded by pouring the MIC into the tube while being vibrated with a Cleveland vibrating block in an attempt to achieve a uniform density without mechanically packing the material. In other experiments, pressed pellets were stacked end to end within the tube instead of pouring the loose powder into the tube. This method allowed for testing these materials at much higher densities than has been considered previously in an instrumented tube test. Pellets used in the high-density shots were pressed to a specific density and then loaded individually into the tube using a remote pellet loading station which is shown in Fig. 2. The assembly was mounted inside of a fragment-containing box with only the slide protruding outside of the box. Loading was achieved by placing a pellet onto the slide and then pushing it through the optical port access hole and into the tube. With this device, tubes can be loaded one pellet at a time up to a total charge weight (material mass) of 5 g. However, the operator is never exposed to more than the mass of a single pellet that for safety reasons is limited to less than 1 g because of the spark and friction sensitivity of these materials. At higher densities, the mass of the charge would have exceeded safe handling restrictions.

In the original design and in our tests performed at low density, a bare electric match head is used to ignite the material. This method led to deviations in ignition time and was therefore modified to incorporate the use of an exploding bridge wire (EBW) as the initiator. The EBW was threaded into a steel adapter which mounted to the end of the block. The configuration is the same as used in a SE-1 detonator. The EBW also served as a stop for the loading of pellets into the tube as it was secured into an adapter that was fastened to the end of the tube block. Ignition with an EBW was used on all of the tubes fired at higher densities. Using this method meant that the initiation end of the tube was sealed and, therefore, pressure was not allowed to escape from the ignition end of the tube. This was not the case with the shots fired at low density because the electric match head was quickly blown out of the tube upon ignition, allowing gas to exit the tube and possibly affecting the initial transient.

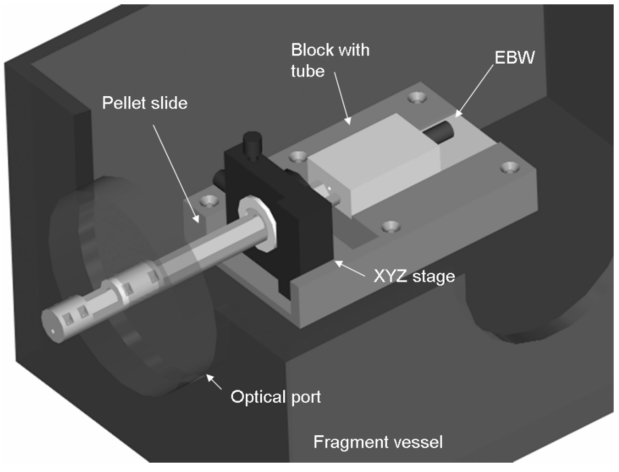

Fig. 2 Rendering of remote pellet loading station within a fragment vessel.

The propagation speed was determined by identifying the time of arrival (5% level of the maximum value) of the light at each optical fiber and then performing a linear regression fit to those points. The same method was used for calculating the propagation speed of the pressure front. The initial transient is observed to be less than a 10th of the tube length for the conditions considered so steady propagation speeds are obtained.

III. Results and Discussion

A. Pressure Cell/Open Tray Experiments

Each of the four oxides was mixed with nanoaluminum and tested in the pressure cell and open burn tray. The samples tested were of bulk (loose powder) density. The measured densities for Al/MoO_3, Al/Bi_2O_3, Al/WO_3, and Al/CuO were 0.498 g/cm^3, 1.24 g/cm^3, 0.522 g/cm^3, and 0.311 g/cm^3 respectively. The ratio of fuel to oxidizer was varied in an attempt to determine an optimum for both propagation speed and peak pressure. Stoichiometry for each system was calculated assuming the following reactions:

$$2Al + MoO_3 \rightarrow Al_2O_3 + Mo \quad (1)$$

$$2Al + Bi_2O_3 \rightarrow Al_2O_3 + 2Bi \quad (2)$$

$$2Al + WO_3 \rightarrow Al_2O_3 + W \quad (3)$$

and

$$2Al + 3CuO \rightarrow Al_2O_3 + 3Cu \quad (4)$$

There is Al_2O_3 in the reactants from the oxide layer in the aluminum that is not shown in the equations for simplicity. These reactions assume completion and do not account for dissociation. We also did not account for the possibility of reaction between the aluminum and gaseous oxidizers such as O_2, N_2, or H_2O. Including the air is not expected to affect results significantly. As evidence, Asay et al. [3] performed tube experiments at atmospheric pressure and in a rough vacuum (3.3 Pa) in which the resulting propagation speeds were nearly identical. The original oxide was included in equilibrium calculations.

Optimization curves for peak pressure and open propagation speed are shown in Fig. 3. The error bars are the standard deviation for three tests performed at each mixture. These experiments reveal that with the exception of Al/CuO, the composites have a ratio considerably fuel rich that produces the higher pressure and therefore faster propagation speed. The composite containing CuO had an optimum ratio near stoichiometric. Similar investigations also report fuel-rich mixtures as being optimum [10–12] although there have been no firm conclusions drawn as to the possible causes. We propose an explanation for this result below.

Recent work by Perry et al. [13] reported the difference in performance between dehydrated WO_3 and $WO_3 \cdot H_2O$. Their data suggest that the water participates in the reaction, and that hydrogen gas is formed in addition to tungsten metal. Rewriting Eq. (3) to account for the reaction with water in the system produces

$$8Al + 3WO_3 \cdot H_2O \rightarrow 4Al_2O_3 + 3W + 3H_2 \quad (5)$$

Despite taking into account the structural water in the oxidizer, the resulting change in stoichiometry is still not equivalent to the optimum ratio we achieved. That is, it is still fuel rich. This is in contrast to the results described by Perry et al. This may indicate that surface H_2O may be present in addition to the chemically structural H_2O. However, in that work, 44 nm aluminum was used which could

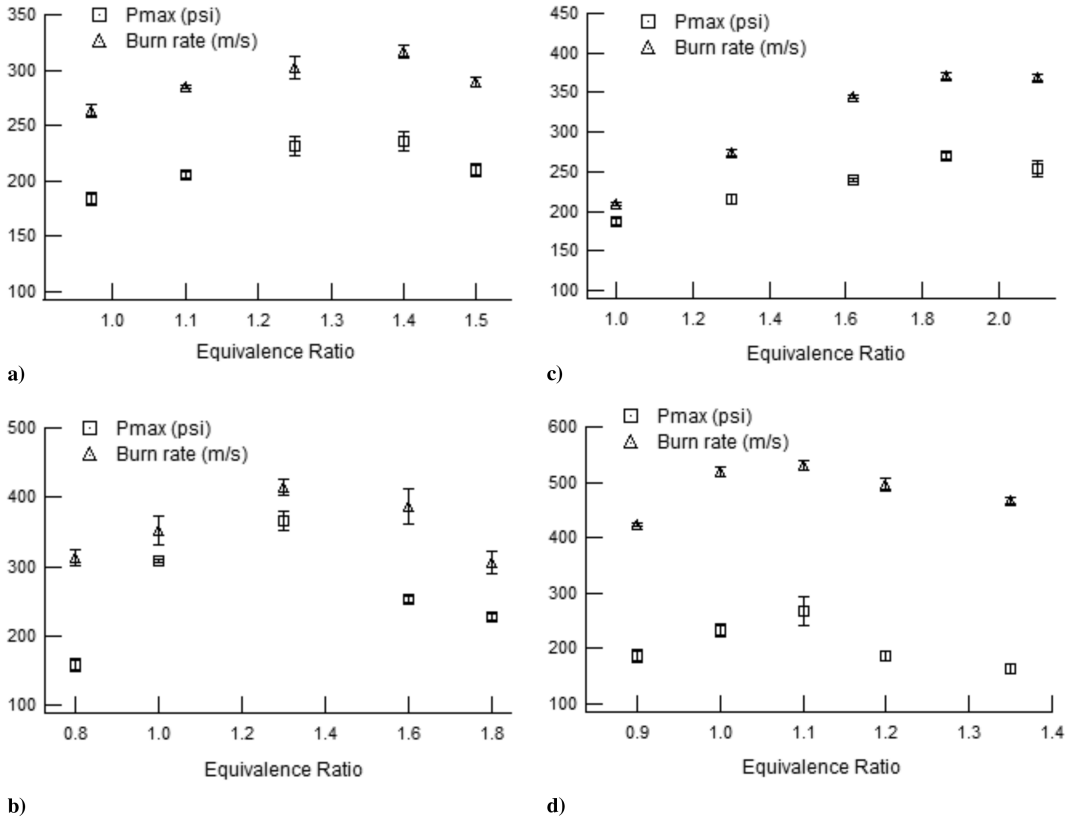

Fig. 3 a) Al/MoO_3, b) Al/Bi_2O_3, c) Al/WO_3, and d) Al/CuO optimization data. Maximum pressures obtained in the reaction cell and propagation speeds (burn rates) are shown.

result in faster reaction rates and therefore could drive the reaction closer to completion. To determine if the other oxides were hydrated, thermogravimetric analysis was performed. The materials were heated to 300°C. This analysis showed no weight loss indicating that no surface or structural water was present.

The data presented in Fig. 3 demonstrate a relationship between pressure output and propagation speed. As observed for each composite, the ratio with the maximum propagation speed in the open tray is also the ratio that produced the maximum peak pressure in the pressure cell experiments. These results show that gas production is important for reaction performance. This is in contrast to normal deflagration where the reaction temperature is more important [14]. For some materials stoichiometric conditions do not produce the most gas.

Chemical equilibrium calculations were performed to help interpret the results. The Cheetah 4.0 [15] program was used. In a recent paper, Hobbs and Baer [16] discussed various product libraries and developed the JCZS product library. Exponential-13,6 (EXP-13,6) potential parameters for 750 gases composed of 48 elements were determined and assembled in a database, referred to as the JCZS database, for use with the Jacobs–Cowperthwaite–Zwisler equation of state (JCZ3-EOS). The "S" refers to Sandia National Laboratory. The Becker–Kistiakowsky–Wilson equation of state (BKW-EOS) is used extensively to calculate detonation properties of condensed explosives [16]. Two different parameterizations of the BKW-EOS are in Cheetah BKWS [17] and BKWC [18]. The "C" and S represent Cheetah parameterization and Sandia parameterization, respectively. Another product library used in Cheetah is EXP6.2. Where possible we compared results between the product libraries and with other equilibrium codes. A constant one-atmosphere pressure problem was assumed.

We found that very fuel-rich cases produced solid Al in the products using BKWS or JCZS (as implemented in Cheetah 4.0) product libraries, although the temperature was far above the melting temperature of Al (933 K) [19]. This is not physically plausible. Both BKWS and JCZS produced similar results for the majority of the conditions considered. JCZS sometimes predicted solid Al in the products at lower fractions of nAl than BKWS. Mel Baer[§] provided the authors with a corrected JCZS library for Cheetah 4.0 that did not exhibit these problems. Therefore, the results presented used this JCZS library.

For the Al/MoO_3 case, using the product library EXP6.2 produced a peak temperature at $=1.01$ (30% mass nAl that is 88% active). The total gas production peaks at $\phi = 1.39$ (37.2% mass nAl) and this peak is much closer to the optimized propagation speed peak (near $\phi = 1.4$). This result suggests that the propagation speeds depend on the gas products. In addition, the optimization for an open burn experiment is similar to the reported optimization in tube experiments using similar materials [20]. This suggests that although the propagation speed differs between the two experiments the modes are likely similar. The differences are likely due to the loss mechanisms between the two experiments, but importantly the underlying mode for the propagation is probably the same. However, these results are based on using the product library EXP6.2 that does not include many aluminum species, such as Al_2O, AlO, etc. In addition, EXP6.2 does not predict the solidification of Mo even though temperatures dropped below the melting temperature of Mo (2896 K) [19]. Clearly, the thermodynamics are too simplified with EXP6.2. Consequently, we used the JCZS product library for the remaining results.

For the Al/MoO_3 case, by using the product library JCZS a peak temperature at $\phi = 1.00$ (30% mass nAl that is 88% active Al) was obtained. Near the mixture ratio where the maximum propagation speed is observed the predicted gas production is not at a maximum, but is still increasing and peaks at a more aluminum rich mixture (about 41% mass nAl). However, at about $\phi = 1.41$ (37.5% mass nAl) in the calculations the solid Mo begins to be predicted in the equilibrium products. This is consistent with the melting temperature of Mo at 2896 K [19] and this equivalence ratio is much closer to the optimized propagation speed peak (near $\phi = 1.4$). The mechanism suggested is that liquid Mo is being propelled forward by hot

[§]Baer, M. R., private communication, 2006.

convective gases and solidifying on unreacted materials. This could greatly enhance a convective heat transfer mode where mass is propelled forward. This method of heat transfer may also contribute to a melt dispersion mechanism proposed by Levitas et al. [21]. Their proposal suggests that during heating, a nanoaluminum particle melts within its oxide shell generating high relative pressures. Upon spallation of the oxide shell, an unloading wave disperses the liquid aluminum. Our proposed mode of heat transfer through liquid Mo could aid in the fast heating needed to support melt dispersion.

Figure 4a shows the calculated results for the Al/Bi_2O_3 composite. Bi boils at 1837 K [19]. The temperature and gaseous Bi peaks near stoichiometric conditions, $\phi = 1$. However, for fuel-rich conditions gaseous species of Al contribute to the overall gaseous species and the total gas production peaks just below $\phi = 1.3$. This is very close to the maximum propagation speed and pressure (see Fig. 3b). Again, this suggests that the propagation speed is dependent on the gas production, consistent with a convective mode. In addition, hot gaseous Bi condensing on unreacted material could augment the convective heat transfer.

Figure 4b shows the calculated results for the Al/CuO composite. Cu boils at 2835 K [19]. As a result of this relatively high boiling temperature, as temperatures drop at ratios deviating from stoichiometric conditions, solid Cu becomes a product. The temperature and gaseous Cu peak near stoichiometric conditions, $\phi = 1$. At more fuel-rich conditions predicted gaseous Al increases, but this is not enough to overcome the loss of gaseous Cu, as more Cu is predicted to be solid. Experimentally, the maximum propagation speed and pressure (see Fig. 3d) occur at slightly fuel-rich conditions, $\phi = 1$. This is close to the predicted peak in gas products, as seen in Fig. 4b.

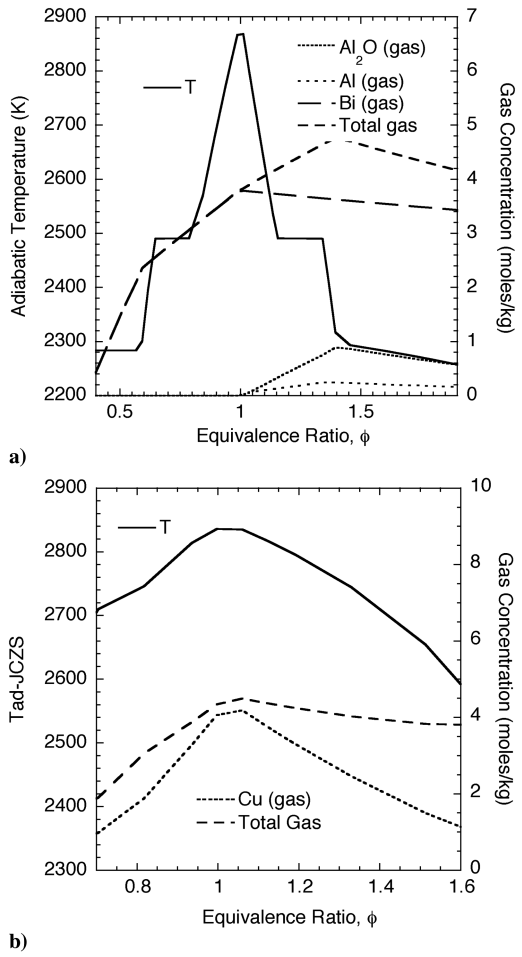

Fig. 4 Equilibrium calculations for a) Al/Bi_2O_3 and b) Al/CuO composites.

Calculations were also made for the $Al/WO_3 \cdot H_2O$ system. The peak in gaseous products is fuel rich, but not as much as observed experimentally. Consequently, we suspect there was some surface absorption of additional H_2O that was not quantified. However, the same qualitative effects are observed. Specifically, that the optimum propagation speed is achieved when the composite is fuel rich. In the future, dehydrated WO_3 should be used.

B. Instrumented Burn Tube Experiments

Experiments were first performed on the four composites at low density and for the Al/MoO_3 and Al/Bi_2O_3 at 47% of theoretical maximum density (TMD). TMD for Al/MoO_3 is 3.808 g/cc and for Al/Bi_2O_3 it is 7.188 g/cc. The other two systems could not be tested at 47% TMD because of inadvertent ignitions while attempting to press pellets at those densities. The low-density loading was achieved using the vibrating method previously reported in Sec. II.C. As shown in Table 2, the densities of the four composites are dissimilar when using this method due to the differences in particle size and morphology of the various oxidizers. Significant distinctions between Al/Bi_2O_3 and the other three systems were observed in these experiments. In particular, when tested at low densities Al/Bi_2O_3 produced significantly higher pressures and lower propagation speeds when compared to the other three composites. Figure 5 shows a pressure record of each composite tested at low densities. The profiles are plotted on the same scale for comparison. As Fig. 5b shows, the pressure output of an Al/Bi_2O_3 composite is significantly higher than the other three. Table 2 also lists values for peak pressure and propagation speed averaged from multiple experiments along with data normalized for the percentage of fuel in each of these tests.

Several methods were used to determine the velocity of the reaction as it propagated from the point of initiation to the end of the tube. As described in the experimental section, the block incorporated both optical fibers and pressure gauges spaced 10 mm apart, set on opposing sides of the block. The pressure gauges were used not only for the recording of pressure but they also allowed us to calculate the velocity based on the time of the initial rise of the signals. This method allowed for some unique observations. In certain cases, a high-speed digital camera was employed to provide a third means of determining propagation speed by tracking the front edge of the visible flame.

The experiments at low densities for composites having MoO_3, WO_3, and CuO revealed that the time of arrival taken from each pressure gauge was slightly later in time than its corresponding optical trace. However, as the reaction propagated along the length of the tube, the difference in time between the two measurements decreased. An example of this behavior is shown in Fig. 6 where time of arrival for both optical and pressure measurements is plotted against distance along the tube. Also plotted is the Δt between the two, which is ~ 9 μs when light is detected at the first point of measurement, then approaches 5 μs as the reaction reaches the last measurement. Because the pressure front and light front are reasonably steady, we calculate the distance between the two fronts to vary from approximately 6.8 mm at the beginning of the tube to 5.8 mm at the end. This particular graph shows data from a test with Al/MoO_3 at low density.

Similar behavior occurred in composites having WO_3 and CuO as the oxidizer. However, in the experiments involving Bi_2O_3, a different behavior was observed. Instead of the pressure wave apparently catching up to the leading edge of the reaction where light is first emitted, the Δt between the two increases along the length of the tube and reaches a near constant value. An example of this is illustrated in Fig. 7. In this test the distance between the two fronts increases from 8.5 mm to nearly 12 mm. In contrast to the apparent convergence of the two fronts at low densities, MoO_3 tested at higher densities produces a behavior similar to the Al/Bi_2O_3 composite. That is, the Δt between the two measurements increases instead of decreasing as was observed at low densities. There are several possible explanations for this behavior. One is that the increase in density inhibits the ability of heat transfer by convective flow (lower

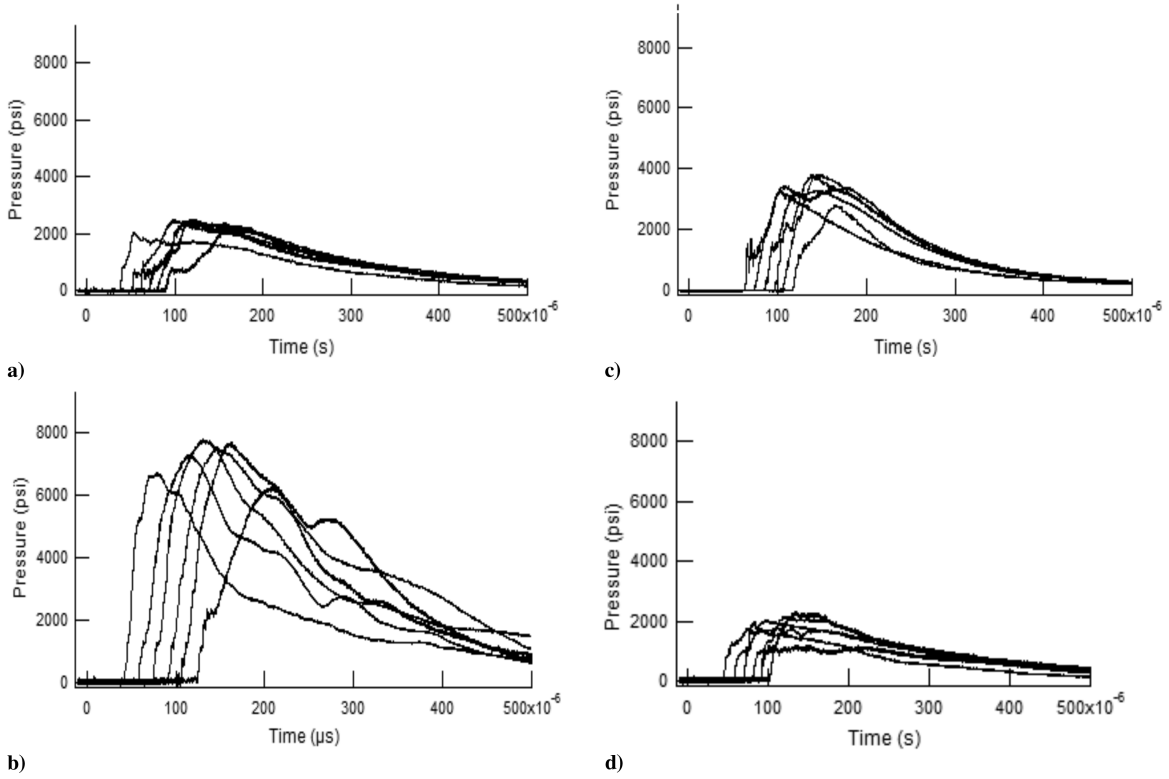

Fig. 5 a) Al/MoO_3, b) Al/Bi_2O_3, c) Al/WO_3, and d) Al/CuO pressure histories from the instrumented burn tube experiment.

permeability) yet increases the contact between particles that increases the transfer of heat by conduction. Given that tests with Al/Bi_2O_3 at all tested densities and MoO_3 at high density show similar behavior, it is possible that the effect is caused by the high output pressures recorded in these tests. As seen in Table [2], the resulting pressures and propagation speeds are similar for both composites at high densities. High-density experiments were not performed with WO_3 or CuO.

Along with the initial increase in separation of the ignition and pressure fronts in the higher density tube tests, we have also observed that the overall propagation speed of the Al/MoO_3 composite decreases with increasing density. A similar trend is seen with Al/Bi_2O_3 composite, but it is less dramatic (see Table 2). This behavior is opposite of a detonating explosive where there is a near linear dependence of detonation velocity upon the initial density of the explosive [22]. Figure 8 shows the trend of higher pressure, lower velocity behavior seen across the range of tested densities with the Al/MoO_3 composite. These data may not reflect the behavior at all possible densities. However, Pantoya and Granier [23] reported a similar behavior in a nanoscale Al/MoO_3 composite when observing the combustion of unconfined (not burned in a tube) pressed pellets across a wider range of densities. This behavior is consistent with a mechanism dominated by convective flow at low density, eventually transitioning to conductive control at much higher densities. Importantly, this trend with density is opposite what occurs for detonations.

The apparent convectively dominated wave propagation at speeds that are supersonic with respect to the sound speed in these materials may be similar to "convective detonation" studied by Ershov [24] for combustion of reactive gases in a porous structure. The convective detonation mode in a porous media can admit supersonic propagation without a conventional shock wave. Instead this mechanism involves a complex wave front made up of hot gaseous jets that protrude randomly from the combustion zone ahead of the average wave front [24].

As further evidence to this, we have also examined high-speed digital photography, which reveals a difference in the propagation of the ignition fronts between low and higher densities. Nearly steady velocities were observed for all four systems along the length of the tubes when fired at low density. Photographic analysis also reveals an uninterrupted, nearly planar burning at the leading edge of the front for the entire length of the reaction. Similar evidence has been reported in other work [3,9]. For tubes at higher densities, more stochastic propagation is observed using all three of our recording techniques. This can be observed directly in high-speed video of the higher density tests. At 47% TMD the propagation is noticeably different than at poured densities. Figure 9 shows four consecutive frames of a reaction within a tube that illustrate a very nonplanar front. The frame rate is 76,000 fps with an interframe time of 13 μs. The ignition front appears to almost skip one section of unreacted material and continues to propagate beyond this section toward the end of the tube. The effect of the interface between pellets may contribute to the nonsteady propagation as well; however, the extent is unknown. Because there must be some tolerance between the outer diameter of the pellets and the inner diameter of the tube, it may be expected that the free volume would result in increased propagation

Table 2 Performance of composites. Average values are from three tests

	Pressure cell P_{avg}, psi	Open tray V_{avg}, m/s	Low density %TMD	Burn tube low density P_{avg}, psi	Burn tube low density V_{avg}, m/s	Burn tube 47% TMD P_{avg}, psi	Burn tube 47% TMD V_{avg}, m/s
Al/MoO_3	240	320	11	2700	950	6595	580
Al/Bi_2O_3	365	425	17	7750	646	5700	560
Al/WO_3	260	365	9	3900	925	[a]	[a]
Al/CuO	250	525	6	1900	802	[a]	[a]

[a]Not tested at 47% TMD.

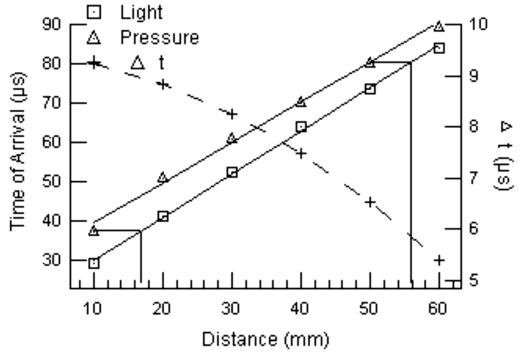

Fig. 6 Low-density test showing converging pressure and ignition fronts.

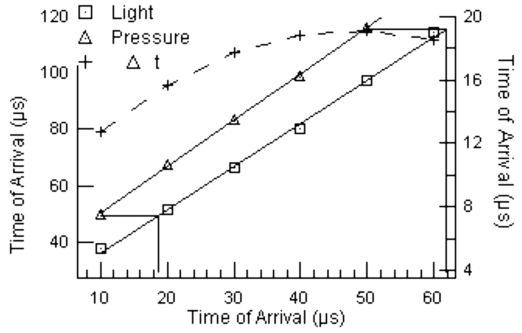

Fig. 7 High-density test showing diverging pressure and ignition fronts.

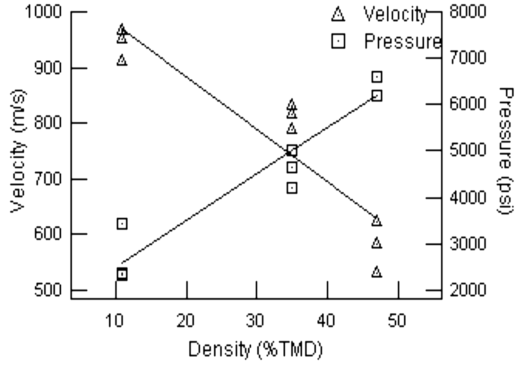

Fig. 8 Al/MoO_3 pressure and velocity vs density.

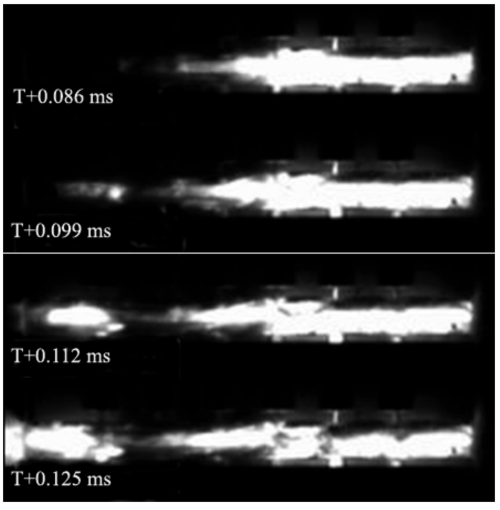

Fig. 9 Images of ignition front in a high-density tube shot.

measurements. Asay et al. [3] observed faster velocities in tube tests with free volume. However, we did not observe any effects on propagation speed that may have been caused by the small tolerance between the pellets and the tube wall.

IV. Conclusions

A method has been developed and implemented for the safe loading and testing of MIC materials at higher charge weights using a remote loading station. While using this technique no inadvertent ignitions of the test material were encountered and much higher densities were achieved.

Quantitative measurements of pressure and propagation speed for four different metal fuel/metal–oxide combinations have been performed. Experimental results demonstrate that each composite behavior has a strong dependence on the metal oxide used. Measurements of the time of arrival of the ignition front and pressure front exemplify the transition from more convectively dominated propagation at low densities to slower convective propagation at higher densities. Both propagations are likely supersonic with respect to the mixture. However, the trends with density are opposite what occurs for detonations. This may indicate that the propagation mode is significantly different than simple detonations. Some have proposed a propagation mode termed convective detonation in multiphase systems. Perhaps this is a form of that mechanism. More work is needed in this area, specifically, testing across a wider range of densities. Theory and modeling work is needed also to fully understand the observed trend with density.

Thermodynamic calculations have helped explain the experimental observations. It is clear for the conditions studied that the propagation speed is dependent on the amount of gaseous species. This correlates with the closed bomb maximum pressure results also. The state of the product metal appears to also be important. For example, liquid Mo appears important in the propagation of Al/MoO_3 composites. The solidification or condensation of the product could greatly enhance heat transfer rates. We have also successfully explained, using equilibrium calculations, why the Al/CuO composite optimized near stoichiometric conditions, instead of fuel-rich conditions. The propagation depends on gas production and the state of the products. Higher gas production and gas or liquid products favor higher propagation speed. This insight will help in the design and use of these composites.

Acknowledgments

This study was performed at the Los Alamos National Laboratory, operated by the University of California for the Department of Energy (DOE) under Contract W-7405-ENG-36. Funding for this work was provided by the Joint Munitions Program (DOE and Department of Defense). The authors would also like to acknowledge Ed Roemer, Bettina Smith, Mary Sandstrom, and Jim Busse for their individual contributions.

References

[1] Aumann, C. E., Skofronick, G. L., and Martin, J. A., "Oxidation Behavior of Aluminum Nanopowders," *Journal of Vacuum Science and Technology B (Microelectronics and Nanometer Structures)*, Vol. 13, No. 3, May 1995, pp. 1178–1183.

[2] Son, S. F., Asay, B. W., Busse, J. R., Jorgensen, B. S., Bockman, B., and Pantoya, M., "Reaction Propagation Physics Of Al/MoO_3 Nanocomposite Thermites," *Proceedings of the 28th International Pyrotechnics Seminar*, International Pyrotechnics Society, Mesa, AZ, Nov. 2001, pp. 4–9.

[3] Asay, B. W., Son, S. F., Busse, J. R., and Oschwald, D. M., "Ignition Characteristics of Metastable Intermolecular Composites," *Propellants, Explosives, Pyrotechnics*, Vol. 29, No. 4, 2004, pp. 216–219.

[4] Armstrong, R., "Models for Gasless Combustion in Layered Materials and Random Media," *Combustion Science and Technology*, Vol. 71, Nos. 4–6, 1990, pp. 155–174.

[5] Puszynski, J. A., "Formation, Characterization, and Reactivity of Nanoenergetic Powders," *Proceedings of 29th International Pyrotechnics Seminar*, International Pyrotechnics Society, Mesa, AZ,

July 2004, pp. 14–19.
[6] Perry, W. L., Smith, B. L., Bulian, C. J., Busse, J. R., Macomber, C. S., Dye, R. C., and Son, S. F., "Nano-Scale Tungsten Oxides for Metastable Intermolecular Composites," *Propellants, Explosives, Pyrotechnics*, Vol. 29, No. 2, 2004, pp. 99–105.
[7] Bockman, B., Son, S. F., Asay, B. W., Busse, J. R., Mang, J. T., Peterson, P. D., and Pantoya, M., "Combustion Performance of Metastable Intermolecular Composites (MIC)," *The 38th JANNAF Combustion Subcommittee Meeting*, FL, Vol. I, Eglin AFB, 2002–0458, 2002.
[8] Valliappan, S., Swiatkiewicz, J., and Puszynski, J. A., "Reactivity of Aluminum Nanopowders with Metal Oxides," *Powder Technology*, Vol. 156, Nos. 2–3, 2005, pp. 164–169.
[9] Bockman, B., Pantoya, M. L., Son, S. F., Asay, B. W,, and Mang, J. T., "Combustion Velocities and Propagation Mechanisms of Metastable Intermolecular Composites," *Journal of Applied Physics*, Vol. 98, No. 6, 2005, p. 064903.
[10] Granier, J. J., and Pantoya, M. L., "Laser Ignition of Nanocomposite Thermites," *Combustion and Flame*, Vol. 138, No. 4, 2004, pp. 373–383.
[11] Plantier, K. B., Pantoya, M. L., and Gash, A. E., "Combustion Wave Speeds of Nanocomposite Al/Fe_2O_3: The Effects of Al/Fe_2O_3 Particle Synthesis Technique," *Combustion and Flame* Vol. 140, No. 4, 2005, pp. 299–309.
[12] Puszynski, J. A., "Reactivity of Nanosize Aluminum with Metal Oxides and Water Vapor," *Materials Research Society Symposium Proceedings*, Vol. 800, Dec. 2003, pp. 223–232.
[13] Perry, W. L., Tappan, B. C., Smith, B. L., Bulian, C. J., Busse, J. R., Sanders, V. E., Arp, Z., and Son, S. F., "The Performance of Aluminum-Tungsten Oxide Hydrate Metastable Intermolecular Composite," Los Alamos Internal Report, LA-CP-06-0292, 2006.
[14] Kuo, K. K., "Detonation and Deflagration Waves of Premixed Gases," *Principles of Combustion*, 2nd ed., Wiley, New York, 2005, Chap. 4, pp. 356–357.
[15] Fried, L. E., Glaesemann, K. R., Howard, W. M., Souers, P. C., and Vitello, P. A., *Cheetah 4.0*, Lawrence Livermore National Laboratory, Livermore, CA, 2004.
[16] Hobbs, M. L., Baer, M. R., and McGee, B. C., "JCZS: An Intermolecular Potential Database for Performing Accurate Detonation and Expansion Calculations," *Propellants, Explosives, Pyrotechnics*, Vol. 24, No. 5, 1999, pp. 269–279.
[17] Hobbs, M. L., and Baer, M. R., "Calibrating the BKW-EOS with a Large Product Species Database and Measured C-J Properties," *Proceedings of the Tenth International Detonation Symposium*, ONR 33395-12, Office of Naval Research, Arlington, VA, 1993, p. 409.
[18] Fried, L. E., and Souers, P. C., "BKWC: An Empirical BKW Parameterization Based on Cylinder Test Data," *Propellants, Explosives, Pyrotechnics*, Vol. 21, No. 4, 1996, p. 215.
[19] Lide, D. R., "Physical Constants of Inorganic Compounds," *Handbook of Chemistry and Physics*, 82nd ed., CRC Press, Boca Raton, FL, 2001, pp. 4-39–4-96.
[20] Son, S. F., Foley, T. J., Yetter, R. A., Wu, M. H., and Risha, G. A., "Combustion of Nanoscale Al/MoO_3 Thermite in Microchannels," *Journal of Propulsion and Power* (to be published).
[21] Levitas, V. I., Asay, B. W., Son, S. F., and Pantoya, M., "Melt Dispersion Mechanism for Fast Reaction of Nanothermites," *Applied Physics Letters*, Vol. 89, No. 7, 2006, p. 071909.
[22] Cooper, P. W., "Real Effects In Explosives," *Explosives Engineering*, VCH Publishers, New York, 1996, pp. 275–293.
[23] Pantoya, M. L., and Granier, J. J., "Combustion Behavior of Highly Energetic Thermites: Nano Versus Micron Composites," *Propellants, Explosives, Pyrotechnics*, Vol. 30, No. 1, Feb. 2005, pp. 53–62.
[24] Ershov, A. P., "Convective Detonation Wave in a Porous Structure," *Combustion, Explosion, and Shock Waves*, Vol. 33, No. 1, 1997, pp. 98–106.

V. Yang
Associate Editor